Proceedings of the European Conference Physics of Magnetism, Poznań 2014

Determination of Exchange and Rotatable Anisotropies in Co_2FeSi/IrMn Exchange Coupled Structures using Broadband Ferromagnetic Resonance

H. Głowiński[a,*], M. Schmidt[a], A. Krysztofik[b], I. Gościańska[b] and J. Dubowik[a]

[a]Institute of Molecular Physics, Polish Academy of Sciences, PL-60179 Poznań, Poland

[b]Faculty of Physics, A. Mickiewicz University, Umultowska 85, PL-61614, Poznań, Poland

We determined exchange $H_{\rm ex}$ and rotatable $H_{\rm rot}$ anisotropy fields of multilayers that comprise 10 nm Co_2FeSi (CFS) layers exchange coupled to 20 nm IrMn layers by using ferromagnetic resonance with a vector network analyzer (VNA-FMR). The multilayer structures consist of IrMn/bottom (b)-CFS/IrMn/middle (m)-CFS/IrMn/top (t)-CFS/IrMn layers so that each CFS layer is surrounded by a pair of IrMn layers. In the structures, the exchange bias field propagates in such a way that $H^{\rm t}_{\rm ex} > H^{\rm m}_{\rm ex} > H^{\rm b}_{\rm ex}$ for the top, middle, and bottom layer, respectively. FMR response measured along the exchange bias (EB) axis consist of only two absorptions related to the (b+m)- and (t)-CFS layers, respectively. Exchange and rotatable anisotropy determined independently from angular and dispersion measurements of the resonance fields are nearly the same. Rotatable anisotropy field scales with the exchange bias field in these complex structures.

DOI: 10.12693/APhysPolA.127.531

PACS: 75.30.Gw, 75.30.Et, 75.60.Jk

Besides the unidirectional (exchange bias) and uniaxial anisotropies, ferromagnetic (FM)/antiferromagnetic (AFM) thin film systems with exchange bias (EB) are characterized by the rotatable anisotropy [1, 2]. Therefore, magnetic properties of EB systems involve the uniaxial anisotropy field $H_{\rm u}$, the exchange bias field $H_{\rm ex}$, and the rotatable anisotropy field $H_{\rm rot}$, which give uniaxial ($\propto \cos 2\theta$), the unidirectional ($\propto \cos\theta$), and isotropic terms, respectively, for the free energy of the magnetization of an EB system. θ is an angle between the direction of magnetic field with respect to a chosen direction in the film plane. The rotatable anisotropy comes from an antiferromagnetic uncompensated spin system, which rotates almost simultaneously with FM magnetization [3]. In the present work we determined, using broadband ferromagnetic resonance (VNA-FMR) [4], the anisotropy fields of multilayer systems that comprise four 20 nm IrMn and three 10 nm Co_2FeSi (CFS) exchange coupled layers. The $L2_1$-ordered Co_2FeSi is one of the half-metallic Heusler alloys [5]. Characterization of the buried layers with EB is important, because they are now commonly applied in complex multilayer nanostructures employing giant magnetoresistance or tunnel magnetoresistance [6].

Multilayer structures consisting of Ta(5 nm)/IrMn/ bottom (b)-CFS /IrMn/ middle (m)-CFS/IrMn/ top (t)-CFS/IrMn/Ta(5 nm) were sequentially deposited onto Si (100) substrates by magnetron sputtering with Ar pressure of 2 mTorr after a base pressure of 2×10^{-7} Torr has been attained. During the growth process, an in-plane magnetic field of 300 Oe was applied in order to induce unidirectional anisotropy at the FM/AFM interfaces. Subsequently, the films were heated from RT to 230 °C and then cooled to RT in a field of 1 kOe to improve EB. X-ray diffraction (XRD) was used to determine (111) texture and the grain sizes of IrMn layers [7]. While intensities of (111) and (200) reflections were roughly the same before annealing, the intensity of (111) reflection increased substantially after annealing, thus confirming a better (111) texture, which enhances EB in FM/IrMn systems [8]. Vibrating sample magnetometry (VSM) was used to obtain the magnetization hysteresis loops of the films. VNA-FMR measurements were performed in the field-sweep mode using a broadband FMR set-up with an Agilent vector network analyzer (VNA) and a coplanar waveguide (CPW).

Typical $M(H)$ loops of our structures are presented in Fig. 1 for a single CFS with no IrMn (dashed lines) and for [CFS/IrMn] (continuous lines) samples. It is clearly seen that for the [CFS/IrMn] system we can identify the three minor loops for the bottom, middle, and top CFS layers. We checked with independent magnetooptical Kerr magnetometry (which is surface sensitive) that the top CFS has the highest EB field (Fig. 6(d) in Ref. [7]). Moreover, the magnetic moments of the individual CFS layers are nearly the same as would be expected from the sample geometry (see the inset in Fig. 1). The large difference in EB between the bottom ($H_{\rm ex} = 30$ Oe) and the top ($H_{\rm ex} = 214$ Oe) CFS layers is the most characteristic feature of our [CFS/IrMn] systems. It would imply that the quality of CFS/IrMn interfaces (resulting in increased number of the pinned AFM spins at the interfaces) is improving during deposition of the subsequent layers. The coercivity of the single CFS layer of

*corresponding author; e-mail: glowinski@ifmpan.poznan.pl

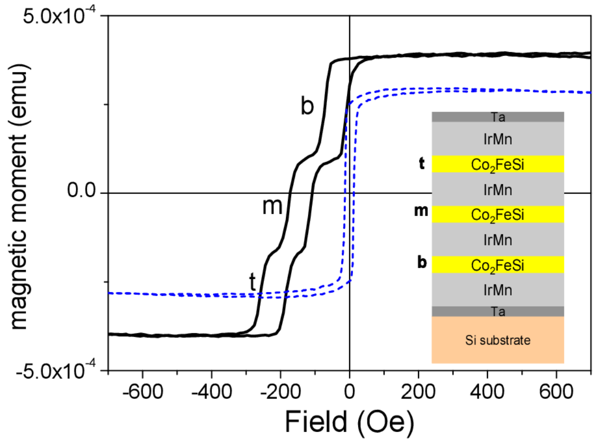

Fig. 1. Typical hysteresis loops of a [CFS/IrMn] multilayer (continues line) and a CFS free layer (dashed line). The inset shows geometry of the CFS/IrMn multilayer.

12 Oe increases to about 30, 30, and 37 Oe for (b)-, (m)- and (t)-CFS, respectively.

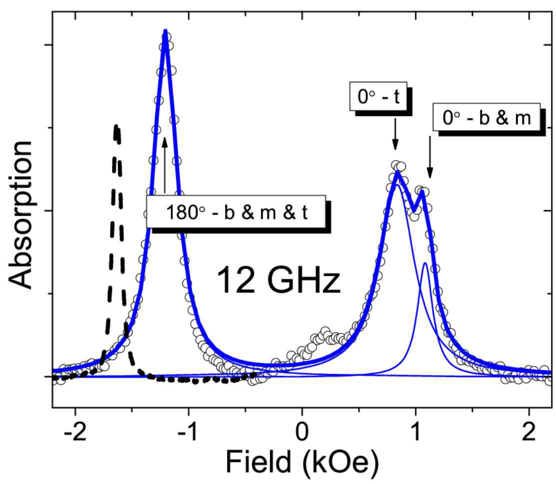

Fig. 2. Ferromagnetic resonance spectra of a typical [CFS/IrMn] multilayer taken along the EB axis (0°) and opposite (180°) to it. The absorptions from the (t)-, (m)-, and (b)-CFS form a single line for 180° and they are partially distinct for 0°. The positive H and negative H correspond to applied fields parallel (0°) and antiparallel (180°) to the EB direction for + and −, respectively. Dashed (black) line shows FMR absorption of an unbiased CFS film.

An example of FMR absorptions of [CFS/IrMn] system, at a driving frequency of 12 GHz, is shown in Fig. 2. EB acts as an effective unidirectional field so that the resonance fields are not equal and correspond to $H(0°)$ and $H(180°)$ for the applied fields parallel and antiparallel to the EB direction, respectively. Moreover, Fig. 2 reveals an asymmetry in the shape of FMR absorption characteristic for the [CFS/IrMn] systems due to the distribution of EB in the bottom, middle and top CFS as it is shown in Fig. 1. Since the IrMn layers are 20 nm thick and effectively decouple CFS layers, one would expect that the FMR signal is triply split. However, the FMR absorption measured for $\theta = 0°$ consist of only two absorptions which can be reasonably related to the (b+m)- and (t)-CFS layers. We argue that this is due to a high FMR linewidth characteristic of the structures with EB. The linewidth of FMR absorption in the free, unbiased CFS film is of 50-80 Oe (Fig. 2). For the typical [CFS/IrMn] structure, the linewidth of the FMR absorption at 12 GHz is of 200-300 Oe, so that we assume that the signals from the (b)- and (m)-CFS are overlapped since $H_{\rm ex}^{\rm b}$ and $H_{\rm ex}^{\rm m}$ are of 30 and 120 Oe , respectively so that $H_{\rm ex}^{\rm m} - H_{\rm ex}^{\rm b}$ is less than the linewidth. On the other hand, the absorption signal forms a single lorentzian peak for $\theta = 180°$.

All the relevant anisotropy fields can be determined using ferromagnetic resonance, which represents a perturbative method for characterization the free energy of the system in the neighborhood of energy minima and involves calculation of an effective free energy of the ferromagnetic film and its derivatives [1]. Following Refs. [1] and [2], the resonance field for a film with EB can be expressed as

$$H_{\rm r}(\theta) = \left\{[2\pi M + \frac{H_{\rm u}}{4}(1+3\cos 2\theta)]^2 + \left(\frac{\omega}{\gamma}\right)^2 - [4\pi M + \frac{H_{\rm u}}{2}(1+\cos 2\theta)] \times H_{\rm u}\cos 2\theta\right\}^{1/2} - 2\pi M - \frac{H_{\rm u}}{4}(1+3\cos 2\theta) - H_{\rm ex}\cos\theta - H_{\rm rot}. \quad (1)$$

For the free CFS film we have a similar expression without the last two terms.

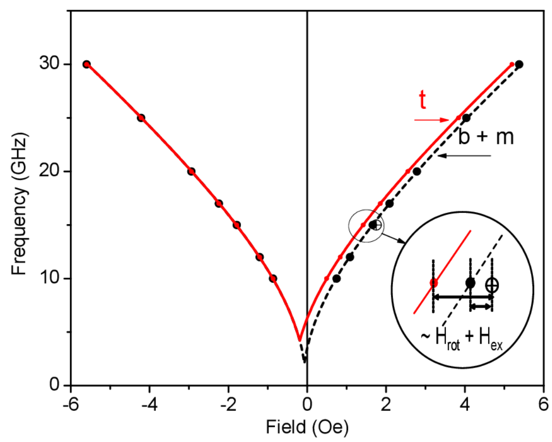

Fig. 3. Ferromagnetic resonance dispersion relations for 0° and 180° (experiment - symbols) and fitting to the experimental data (lines) for a typical [CFS/IrMn] multilayer system.

Figure 3 presents the field dependencies of the FMR frequencies (dispersion relations) for the (b+m)- and (t)-CFS layers (black and red dots). The experimental results were taken at $\theta = 0°, 180°$ and at $90°, 270°$ (not shown) with respect to the EB direction. The continuous lines represent the corresponding calculated numerically fitting curves derived from Eq. (1) for $\theta = 0°$ and $180°$, respectively. The fitting parameters are listed in Table.

An additional experimental data point (shown in Fig. 3 as a crossed circle) represents the resonance field of free CFS film at 12 GHz. The inset shows approximate relation describing the shift of resonance field relative to H_r of the free layer.

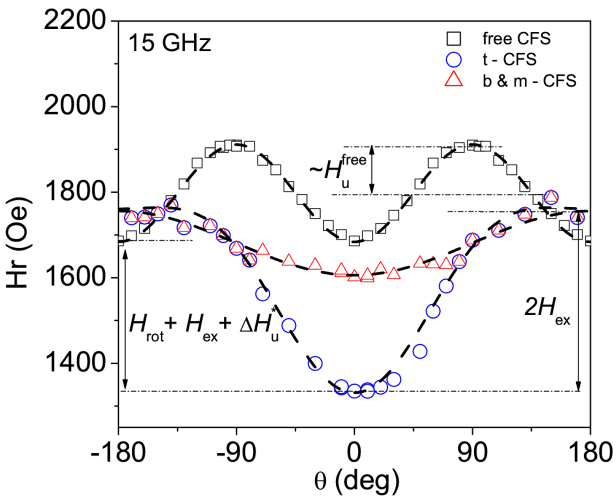

Fig. 4. Angular dependencies of the resonance field of the typical [CFS/IrMn] multilayer and a reference CFS free layer with no EB.

Figure 4 shows angular dependencies of resonance field for the (b+m)-CFS, (t)-CFS layers and the free CFS film measured at 15 GHz. As it was shown in Ref. [1], a shift of resonance field between the (t)-CFS and the free layer is described by approximate relation $H_{rot} + H_{ex}$. The layers (b) and (m) are indistinguishable in FMR measurements because the resonance absorptions are wide, and a shift between them is lower than the linewidth (see Table). Absorptions of (b+m)-CFS and (t)-CFS layers are distinguishable only in a range of angles near 0° since the shift between the FMR absorptions in this region is the highest. Dashed lines are the fittings to the experimental results according to Eq. (1) with the parameters shown in Table. To sum up the FMR experimental results, it is worth mentioning that the values of all anisotropy fields (H_{ex}, H_u, H_{rot}) determined from dispersion relations $\omega(H_r)$ for $\theta = 0°$, 180° and for 90°, 270° (not shown) are in good agreement with the values determined from the angular variations in the resonance field for the [CFS/IrMn] and the free, uncoupled CFS film.

TABLE

Magnetization and magnetic anisotropy fields of the bottom (b), middle (m) and and top (t) CFS layers in the [CFS/IrMn] multilayer system.

Layer	M	H_{ex}^{VSM}	H_C^{VSM}	H_{ex}^{FMR}	H_u^{FMR}	H_{rot}^{FMR}
	[G]	[Oe]				
(b)-CFS	970	30	30	72	24	80
(m)-CFS	970	140	30			
(t)-CFS	960	214	37	190	39	148
free	980	0	12	0	118	0

A striking feature is that the rotatable anisotropy field H_{rot} scales up with H_{ex}. According to a realistic model for polycrystalline exchange-coupled systems [3] the uncompensated interface spins can be classified as unstable (rotatable, responsible for a coercivity enhancement) and stable (i.e., adding to EB). In agreement with Ref. [3], we showed (Fig. 1 and Table) that the number of the stable spins increases from the bottom to the top CFS layer. Hence, the number of unstable spins (resulting in the rotatable anisotropy) should equivalently decrease. The trend observed in our [CFS/IrMn] structures is quite opposite: H_{rot} increases with the increase in H_{ex}. Therefore, it seems that the observed propagation of EB in the [CFS/IrMn] multilayer systems is accompanied with a similar growth in H_{rot} in contrast to Fig. 1 in Ref. [3].

In this work, we showed how to determine the anisotropy fields in the complex multilayer systems. In particular, we showed that ferromagnetic resonance applied for EB systems has rather low field resolution due to a significant broadening of the absorption spectra. Therefore, the FMR absorptions of (b)-CFS overlap with that of (m)-CFS layers. Nevertheless, all relevant anisotropy fields characterizing our complex [CFS/IrMn] with EB can be determined with a good accuracy using both $\omega(H_r)$ data measured along the principal directions with respect to the EB axis and from the data obtained from angular dependencies of the resonance fields (Table). The values of H_{ex}^{FMR} determined from FMR measurements are consistently lower than that determined with VSM in agreement with Ref. [1]. The rotatable anisotropy field H_{rot} and exchange bias field H_{ex} can be used as a measure of unstable and stable spins, respectively. Contrary to our expectations H_{rot} increases with increasing H_{ex}.

References

[1] R.D. McMichael, M.D. Stiles, P.J. Chen, W.F. Egelhoff, *Phys. Rev.* B**58**, 8605 (1998).

[2] B.K. Kuanr, S. Maat, S. Chandrashekariaih, V. Veerakumar, R.E. Camley, Z. Celinski, *J. Appl. Phys.* **103**, 07C107 (2008).

[3] A. Harres, J. Geshev, *J.Phys.: Cond. Matt.* **24**, 326004 ((2012).

[4] C. Bilzer, T. Devolder, J.-V. Kim, C. Chappert, M. Ruehrig, L. Baer, *J. Appl. Phys.* **106**, 063918 (2009).

[5] S. Wurmehl, G.H. Fecher, H.C. Kandpal, V. Ksenofontov, C. Felser,H.-J. Lin, J. Morais, *Phys. Rev. B* **72**, 184434 (2005).

[6] *Handbook of Spin Transport and Magnetism*, Eds.: E.Y. Tsymbal, E.I. Zutic, Chapman Hall/CRC, London 2011.

[7] J. Dubowik, I. Gościańska, K. Załęski, H. Głowiński, Y. Kudryavtsev, A. Ehresmann, *J. Appl. Phys.* **113**, 193907 (2013).

[8] N.P. Aley, M. Bowes, R. Kröger, K. O'Grady, *J. Appl. Phys.* **107**, 09D722 (2010).